Nonlocal Structural Perturbations in a Mutant Human Insulin: Sequential Resonance Assignment and ^{13}C-Isotope-Aided 2D-NMR Studies of [PheB24→Gly]Insulin with Implications for Receptor Recognition†

Qing Xin Hua,‡,§ Steven E. Shoelson,‖ and Michael A. Weiss*,‡,⊥

Department of Biological Chemistry and Molecular Pharmacology, Harvard Medical School, Boston, Massachusetts 02115, Joslin Diabetes Center and Department of Medicine, Brigham and Women's Hospital, Harvard Medical School, Boston, Massachusetts 02215, and Department of Medicine, Massachusetts General Hospital, Harvard Medical School, Boston, Massachusetts 02114

Received August 3, 1992

ABSTRACT: Insulin's mechanism of receptor binding is not well understood despite extensive study by mutagenesis and X-ray crystallography. Of particular interest are "anomalous" analogues whose bioactivities are not readily rationalized by crystal structures. Here the structure and dynamics of one such analogue (GlyB24-insulin) are investigated by circular dichroism (CD) and isotope-aided 2D-NMR spectroscopy. The mutant insulin retains near-native receptor-binding affinity despite a nonconservative substitution (PheB24→Gly) in the receptor-binding surface. Relative to native insulin, GlyB24-insulin exhibits reduced dimerization; the monomer (the active species) exhibits partial loss of ordered structure, as indicated by CD studies and motional narrowing of selected ^1H-NMR resonance. 2D-NMR studies demonstrate that the B-chain β-turn (residues B20–23) and β-strand (residues B24–B28) are destabilized; essentially native α-helical secondary structure (residues A3–A8, A13–A18, and B9–B19) is otherwise maintained. ^{13}C-Isotope-edited NOESY studies demonstrate that long-range contacts observed between the B-chain β-strand and the α-helical core in native insulin are absent in the mutant. Implications for the mechanism of insulin's interaction with its receptor are discussed.

How insulin binds to its receptor poses a problem of general interest. Do conformational changes in the hormone accompany receptor binding, and if so, what structural features are recognized by the insulin receptor? Studies of active analogues containing C-terminal deletions in the B-chain have focused attention on the B-chain β-strand (residues B24–B28) as a possible site of conformational change (Fischer et al., 1985; Nakagawa & Tager, 1986, 1987; Casaretto et al., 1989; Schwartz et al., 1989). Evidence for the functional importance of flexibility in this region has been provided by studies of analogues containing cross-links between the A- and B-chains (Brandenburg et al., 1972; Cutfield et al., 1981; Nakagawa & Tager, 1989; Brems et al., 1991). Of particular interest is mini-proinsulin, an inactive insulin analogue that contains a peptide bond between the B- and A-chains (LysB29–GlyA1; Markussen, 1985). Despite its complete loss of activity, the crystal structure of mini-proinsulin is identical to that of native insulin (Derewenda et al., 1991). Such discordance between function and structure suggests that the various crystal structures of native insulin (Adams et al., 1969; Peking Insulin Structure Group, 1971; Blundell et al., 1972; Bentley et al., 1978; Smith et al., 1984; Baker et al., 1988; Derewenda et al., 1989; Badger et al., 1991) also depict inactive conformers. Derewenda et al. (1991) have thus proposed that the extent of conformational change in the insulin–receptor complex must exceed the range of structural variation among different crystal forms (Dodson et al., 1979; Cutfield et al., 1981; Chothia et al., 1983).

To complement crystallographic studies, we and others have used 2D-NMR[1] spectroscopy to investigate the structure of insulin or insulin analogues in solution (Weiss et al., 1989; Kline & Justice, 1990; Boelens et al., 1990; Hua & Weiss, 1990, 1991; Kristenson et al., 1991; Knegtel et al., 1991; Hua et al., 1991, 1992). Comparative NMR studies of analogues with enhanced or reduced affinity for the insulin receptor would be expected to provide new insights into the mechanism of receptor binding. In this paper we focus on [PheB24→Gly]-insulin, whose "anomalous" near-native bioactivity seems inconsistent with models of insulin receptor-binding based on crystal structures (Mirmira & Tager, 1989). Remarkably, an overall loss of ordered structure in the mutant protein is observed by circular dichroism. Corresponding perturbations in structure and dynamics are observed by T_2 relaxation studies (motional narrowing) and 2D-NMR spectroscopy. These perturbations are localized to the C-terminal region of the B-chain (residues B20–B30) and lead in turn to global changes in the predicted receptor-binding surface. We propose that the solution structure of GlyB24-insulin provides a model for

† Supported by grants from the American Diabetes Association (S.E.S. and M.A.W.), Juvenile Diabetes Foundation International (S.E.S. and M.A.W.), NSF (S.E.S.), and NIH (M.A.W.). The Harvard Medical School NMR Facility is supported by NIH 1 S10 RR04862-01. Insulin analogues were prepared with the assistance of a Joslin Diabetes Center DERC grant (DK36836).

* Address correspondence to this author at the Department of Biological Chemistry and Molecular Pharmacology, Harvard Medical School, Boston, MA 02115.

‡ Department of Biological Chemistry and Molecular Pharmacology, Harvard Medical School.

§ Permanent address: Institute of Biophysics, Academia Sinica, Beijing, China.

‖ Joslin Diabetes Center and Department of Medicine, Brigham and Women's Hospital, Harvard Medical School.

⊥ Department of Medicine, Massachusetts General Hospital, Harvard Medical School.

[1] Abbreviations: CD, circular dichroism; DQF-COSY, double-quantum-filtered correlated spectroscopy; DG, distance geometry; DPI, des-pentapeptide(B26–B30)-insulin, HMQC, heteronuclear multiple-quantum coherence; NMR, nuclear magnetic resonance; NOE, nuclear Overhauser enhancement, NOESY, NOE spectroscopy; TFA, trifluoroacetyl; TOCSY, total correlation spectroscopy.

0006-2960/92/0431-11940$03.00/0

sites of conformational change in the hormone–receptor complex with possible application to analogue and drug design (Brange et al., 1988; Markussen et al., 1988).

MATERIALS AND METHODS

Semisynthesis of GlyB24-Human Insulin and ^{13}C-Labeled GlyB24-Human Insulin. *t*-Boc-*O*-benzyl-L-[*ring*-$^{13}C_4$]tyrosine, *t*-Boc-L-[*ring*-$^{13}C_6$]phenylalanine, and *t*-Boc-[1,2-$^{13}C_2$]glycine were purchased from Cambridge Isotope Laboratories (Woburn, MA). Additional unlabeled protected amino acids and reagents were purchased from Applied Biosystems; solid-phase syntheses were performed on an Applied Biosystems Model 430A synthesizer as described (Shoelson et al., 1992). Des-octapeptide human insulin was kindly provided by R. E. Chance (Eli Lilly & Co., Indianapolis, IN). Semisynthesis of GlyB24-insulin from DOI and the corresponding protected octapeptide [NH-Gly-Gly-Phe-Tyr-Pro-Lys(Boc)-Thr-OH] was accomplished in trypsin-catalyzed reaction as described (Inouye et al., 1979, 1982; Shoelson et al., 1983b, 1992; Nakagawa & Tager, 1986). The analogue was purified as described (Shoelson et al., 1992) and characterized by amino acid composition and HPLC. Incorporation of ^{13}C-labels into GlyB24-insulin was verified by NMR (below).

CD. Spectra were obtained at 25 °C using an Aviv spectropolarimeter with a 1-mm path length cuvette. The protein concentration (determined by absorbance at 280 nm) was 25 μM; native insulin is primarily but not completely monomeric under these conditions. Ellipticity was measured for 10 s at each nanometer; final spectra were smoothed by averaging adjacent points.

NMR. Spectra were recorded at 500 mHz at Harvard Medical School. A total of 2048 points were sampled in t_2; 400 t_1 values were obtained, and the data matrix was zero-filled to 2K × 2K. TOCSY and NOESY spectra were processed using shifted sine-bell window functions with exponential apodization in both dimensions; DQF-COSY spectra were processed similarly, with the addition of a squared sine-bell function. ^{13}C-Isotope-edited experiments were performed as described by Bax and Weiss (1987); ^{13}C decoupling was accomplished during ^1H acquisition using the WALTZ-16 scheme. Carr–Purcell–Meiboom–Gill (CPMG) studies of T_2 relaxation times were performed with 16 transverse delay times in the range 0–1.20 s; the data was fit to a single exponential decay with the time constants as given in Tables III and IV.

RESULTS

(I) Overall Features of Circular Dichroic and ^1H-NMR Spectra

Circular Dichroism. In Figure 1A are shown far-UV CD spectra of native insulin (solid line) and GlyB24-insulin (dashed line). Attenuation in mean residue ellipticity is observed at wavelengths (205–230 nm) sensitive to formation of secondary structure. These changes suggest substantial loss of ordered structure in the mutant protein. Because partial attenuation of such CD bands can be observed on dissociation of insulin dimers into monomers (Melberg & Johnson, 1990), control studies of PheB24 and GlyB24 analogues were conducted in an engineered insulin monomer (Figure 1B) (Weiss et al., 1991; Shoelson et al., 1992). Similar attenuation of structure-sensitive CD bands is observed, indicating that GlyB24 perturbs the structure of the monomer. GlyB24-insulin may also exhibit reduced dimerization, as suggested by the small difference in the extent of attenuation in the two CD studies.

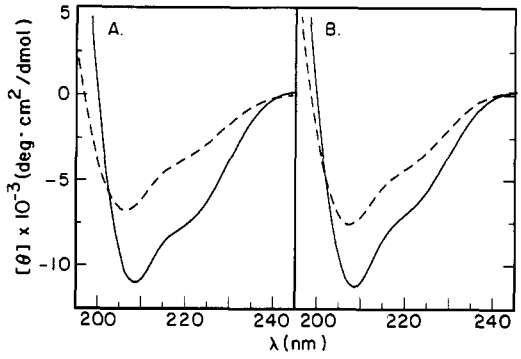

FIGURE 1: (A) Far-UV CD spectra of native human insulin (solid line) and GlyB24-insulin (dashed line) in aqueous–HCl solution (pH 1.9) at 25 °C. (B) Corresponding CD spectra of monomeric insulin analogue (DKP-insulin; Weiss et al., 1991) containing PheB24 (solid line) and GlyB24 (dashed line) under similar conditions. Similar attenuation of mean residue ellipticity is observed at pH 7.4. In each case the protein concentration was 100 μM. DKP-insulin contains the substitutions HisB10Asp, ProB28Lys, and LysB29Pro.

Solvent Conditions for NMR Study. Native insulin forms dimers and higher-order oligomers in aqueous–HCl solution (Goldman & Carpenter, 1974). Accordingly, the present 2D-NMR studies are conducted primarily in 20% deuteroacetic acid, conditions under which native insulin is monomeric and stably folded (Weiss et al., 1989; Hua & Weiss, 1991). Although GlyB24-insulin was not designed to be monomeric, NMR studies in 0–20% deuteroacetic acid (see below) indicate that the analogue is in fact monomeric in aqueous–HCl solution (pH 1.8). Accordingly, ^1H-NMR studies of GlyB24-insulin may be conducted both in 20% deuteroacetic acid and in aqueous–HCl solution (pH 1.8). The former conditions permit effects of the mutation to be determined relative to native insulin, and the latter provide a control for solvent composition.

1D ^1H-NMR Studies. Spectra of GlyB24-insulin and native insulin in aqueous–HCl solution (pH 1.8) and in 20% deuteroacetic acid are shown in Figure 2 (left-hand box). We first compare the spectra of the native and mutant proteins in aqueous–HCl solution. The arrow and asterisk (panels A and D) indicate tyrosine resonances in the B-chain (B16 and, to a lesser extent, B26) whose linewidths are sensitive to dimerization (Weiss et al., 1989). These resonances are sharp in the spectrum of GlyB24-insulin (panel A) but broadened by intermediate exchange in the spectrum of native insulin (panel D). Such differences are seen more clearly in DQF-COSY spectra; antiphase cancellation of broad resonances in the native spectrum leads to disappearance of the TyrB16 and PheB24 aromatic cross-peaks and to attenuation of the TyrB26 cross-peak (supplementary material). Such broadening is not observed in 20% deuteroacetic acid, in which the native and mutant proteins are each monomeric.

Motional Narrowing and Chemical-Shift Dispersion. Inspection of the ^1H-NMR spectrum of GlyB24-insulin suggests two subclasses of spin systems: (a) resonances whose linewidths and secondary shifts are similar to those of corresponding resonances in native insulin, and (b) resonances whose linewidths and secondary shifts are *significantly smaller* than those of corresponding resonances in native insulin. The existence of these subclasses suggests that loss of ordered structure (as inferred from circular dichroism) occurs in a discrete region of the protein as analyzed further below (part II).

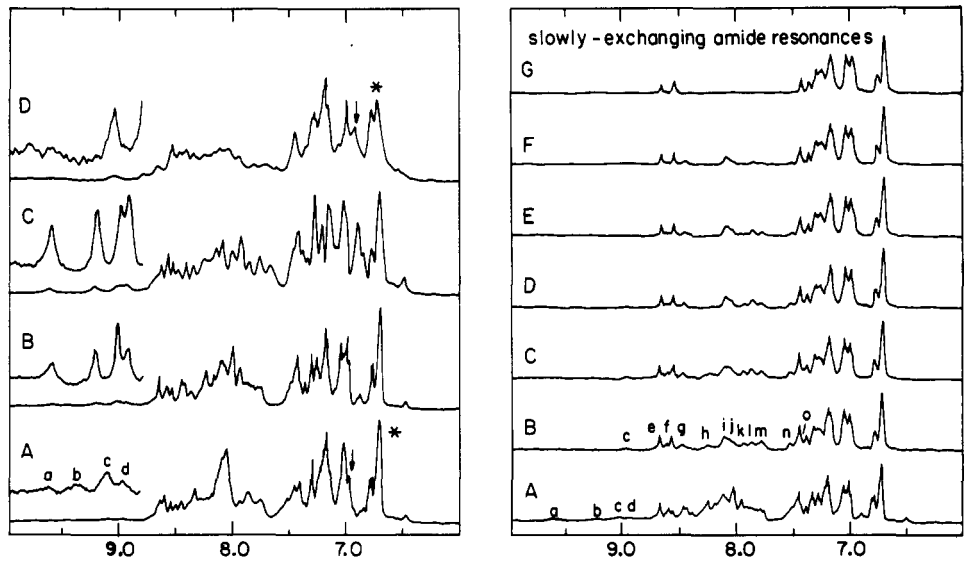

FIGURE 2: (Left-Hand Panel) (A) One-dimensional ^{1}H-NMR spectrum of GlyB24-insulin in aqueous solution (pH 1.8). Downfield amide resonances a–d are assigned to A11, B8, B9, and B6, respectively (inset × 10). (B) ^{1}H-NMR spectrum of GlyB24-insulin in 20% acetic acid. (C) ^{1}H-NMR spectrum of native human insulin in 20% acetic acid. (D) ^{1}H-NMR spectrum of native human insulin in aqueous solution (pH 1.8) exhibits extensive intermediate-exchange broadening due to self-association (Weiss et al., 1989). Arrows and asterisks in panels A and D indicate resonances of TyrB26 (which overlap other aromatic resonances in each case). The B26 resonances are very sensitive to partial dimer formation, since the B26 ring packs in the dimer interface. These resonances are broadened in native insulin (D), but not in the spectrum of GlyB24-insulin (A). In each case the protein concentration was ca. 1.5 mM. (Right-Hand Panel) Slowly-exchanging amide resonances of GlyB24-insulin in 20% acetic acid demonstrate the stability of the α-helices over 12 h; corresponding exchange in native insulin is 3-fold slower (Hua & Weiss, 1990, 1991a,b). (A) Base-line ^{1}H-NMR spectrum of GlyB24-insulin in 80% H_2O/20% deuterated acetic acid. (B) ^{1}H-NMR spectrum of GlyB24-insulin 10 min after dissolution in 80% D_2O/20% deuterated acetic acid. (C–G) Successive time points are 20 min, 40 min, 60 min, 2 h, and 12 h, respectively. Resonance assignments in panels A and B: (a) A11, (b) B8, (c) B9, (d) B6, (e) A12 and B19, (f) A13, (g) A2 and B18, (h) A6 and A7, (i) A4, A16, A17, B15, and B16, (j) B10, (k) B13, (l) A19 and B17, (m) A10 and B14, (n) A14 and A15, and (o) A18.

Conformational Broadening of Amide Resonances. As in the ^{1}H-NMR spectrum of native insulin (Weiss et al., 1989; Kline & Justice, 1990), differential broadening of amide resonances is observed in the spectrum of GlyB24-insulin and ascribed to exchange among conformational substates (Figure 2, left-hand panel). Presumably, collective motions in native insulin responsible for conformational broadening are retained on a similar time scale in the mutant protein. Such motions do not require the breakage of hydrogen bonds, as indicated by the observation of slowly-exchanging amide resonances (Figure 2, right-hand panel). Conformational broadening is more severe in aqueous–HCl solution than in 20% deuteroacetic acid (Figure 2, left-hand panel) as illustrated by the four amide resonances resolved in the downfield region (CysA11, GlyB8, SerB9, and LeuB6; labeled a–d in spectrum A).

(II) 2D ^{1}H-NMR Studies in 20% Acetic Acid

Sequential assignment is first obtained in 20% deuteroacetic acid and extended to aqueous–HCl solution in part III. The primary structures of the A- and variant B-chains of GlyB24-insulin are shown in Figures 3 and 4, respectively. The A-chain contains 21 residues, and the B-chain contains 30 residues. Spin-system classification is accomplished by analysis of DQF-COSY and TOCSY spectra; representative TOCSY spectra of GlyB24-insulin are shown in Figure 5 in 20% deuteroacetic acid (panels A and C) and aqueous–HCl solution (panels B and D). In either solvent a single spin system is observed for each residue.

Sequential Assignment. H_N–H_α ("fingerprint") and H_N–H_N regions of the NOESY spectrum of GlyB24-insulin in 20% deuteroacetic acid are shown in Figure 6. Sequential and medium-range contacts are shown separately for the A-chain (panels A and C) and B-chain (panels B and D). A

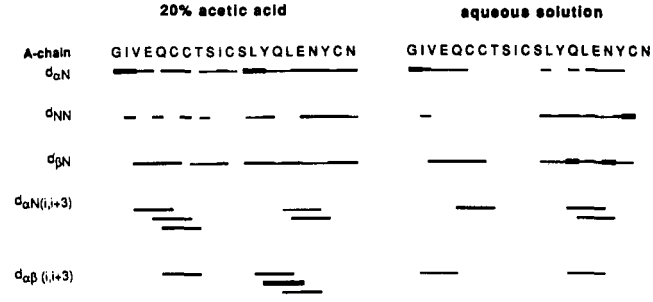

FIGURE 3: Summary of sequential and medium-range connectivities in the A-chain in 20% acetic acid (left) and aqueous solution at pH 1.8 (right). The format and symbols are as developed by Wuthrich (1982, 1986). Analogous data for native insulin have been published (Hua & Weiss, 1991b).

summary of sequential and medium-range NOEs is provided in schematic form (Wuthrich, 1986) in Figures 3 (A-chain) and 4 (B-chain). Because fingerprint NOEs may be attenuated both by amide broadening (in the folded region of the protein) and local dynamics (in unfolded regions), interpretation of their relative intensities is not straightforward. Complete assignment of ^{1}H-NMR resonances is obtained and given in Table I; differences from native insulin (>0.1 ppm) are given in Table II. Motional narrowing and loss of secondary shifts involving residues B20–B30 are described in turn.

(i) Motional Narrowing. Because cross-peak intensities in DQF-COSY spectra are sensitive to the dimensionless ratio $\Delta\omega/J$ (Weiss et al., 1984), their comparison in the spectra of native and mutant insulins provides a qualitative indication of changes in resonance linewidth and (in the absence of intermediate-exchange mechanisms) of relative mobilities. In Figure 7 are shown slices through representative DQF-COSY multiplets assigned to the B-chain. Relative narrowing is

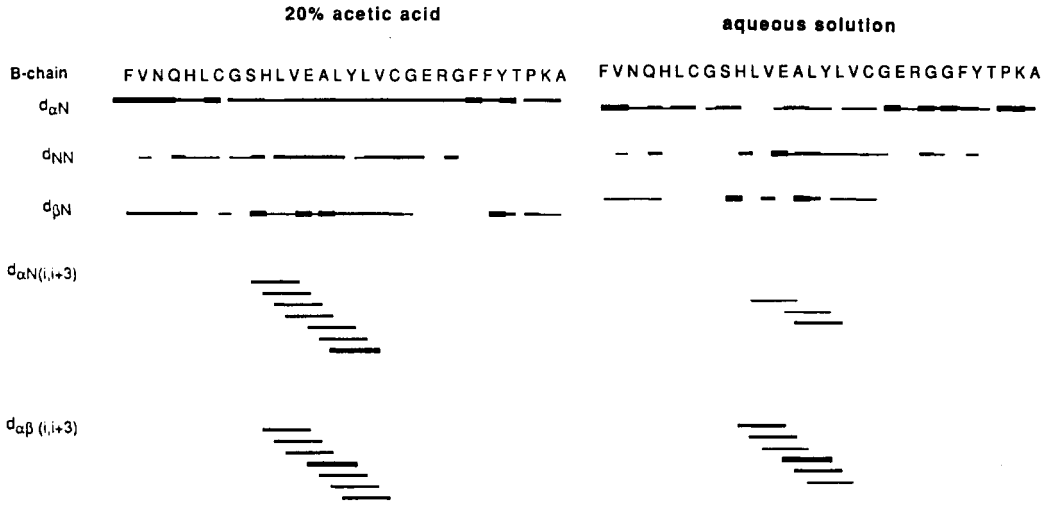

FIGURE 4: Summary of sequential and medium-range connectivities in the B-chain in 20% acetic acid (left) and aqueous solution at pH 1.8 (right). The format and symbols are as described in Figure 3.

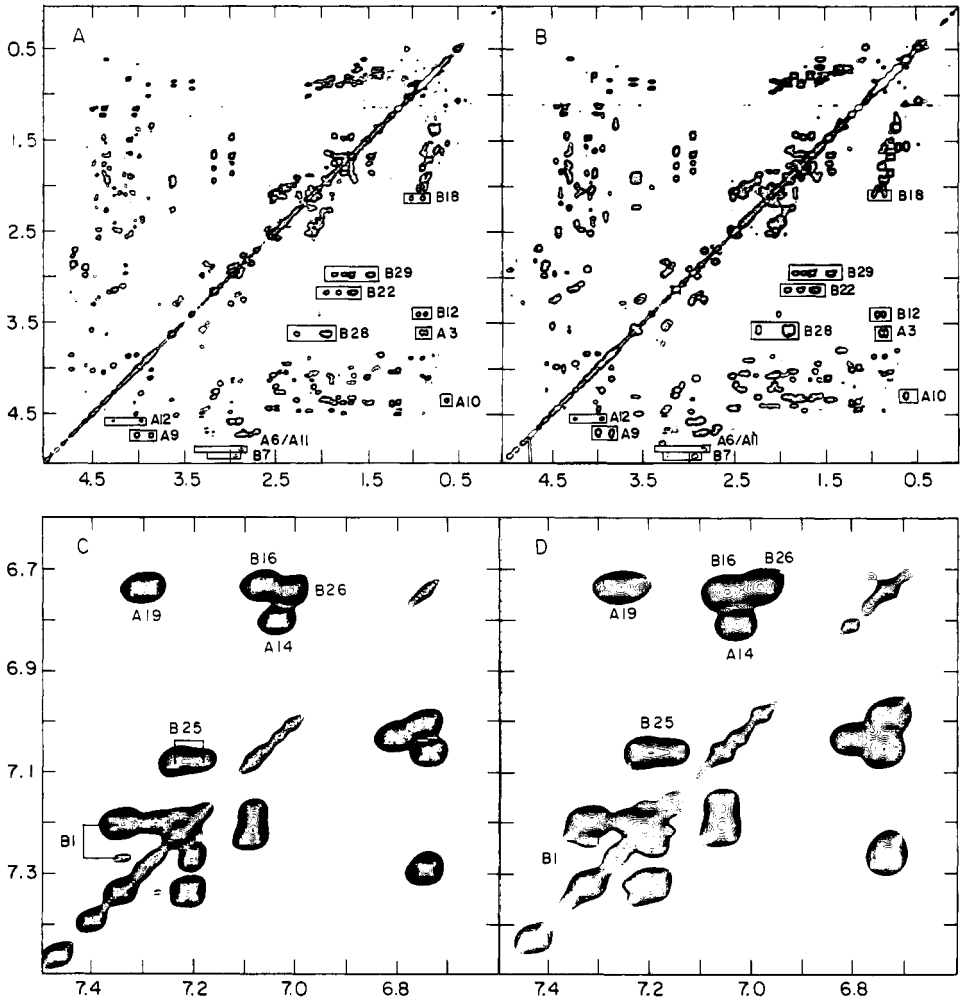

FIGURE 5: Comparison of TOCSY spectra of GlyB24-insulin in 20% acetic acid (panels A and C) and in aqueous solution (panels B and D). A general correspondence of spin-system chemical shifts is observed. Selected aliphatic spin systems are labeled in panels A and B. Enlargement of the aromatic regions is shown in panels C and D with assignments indicated.

observed involving residues in the C-terminal region of the B-chain (B22–B30). Resonances assigned to the side chains of ValB12 and LeuB15 are also narrowed in the spectrum of the mutant protein; in native insulin these side chains pack against PheB24 and TyrB26. Their greater mobility in the mutant presumably reflects loss of such long-range side-chain interactions. In Figure 8 are shown corresponding A-chain DQF-COSY multiplets. Although cross-peak intensities are similar in the two cases, relative narrowing of C-terminal $\alpha\beta$ cross-peaks (GlnA15, AsnA18, and TyrA19) is observed in the spectrum of GlyB24-insulin. In native insulin this region packs against side chains of the B-chain α-helix (including LeuB15).

Measurement of nonselective spin–spin relaxation times (T_2) complements qualitative analysis of DQF-COSY multiplet intensities to provide evidence of motional narrowing.

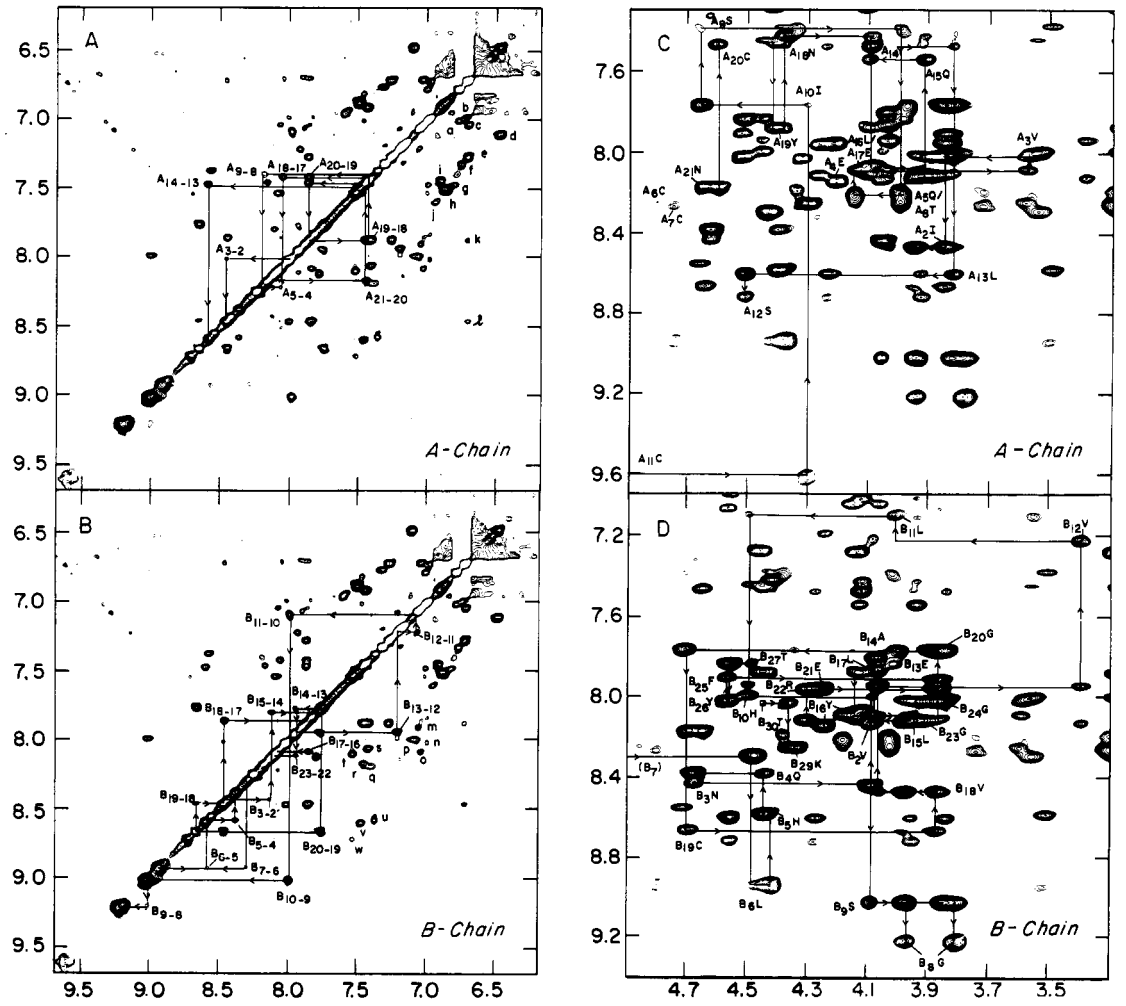

FIGURE 6: Sequential assignment of GlyB24-insulin in 20% acetic acid. Connectivities in the A- and B-chains are shown separately: (A) d_{NN} connectivities in the A-chain, (B) d_{NN} connectivities in the B-chain, (C) $d_{\alpha N}$ connectivities in the A-chain "fingerprint" region, and (D) $d_{\alpha N}$ connectivities in the B-chain "fingerprint" region. Additional resonances in panels A and B are labeled as follows. Panel A: (a) TyrA14-H_δ to -H_ϵ, (b) TyrB26-H_δ to -H_ϵ, (c) TyrB16-H_δ to -H_ϵ, (d) AsnA18-$H_{\delta 1NH}$ to -$H_{\delta 2NH}$, (e) TyrA19-H_δ to -H_ϵ, (f) GlnB4-$H_{\epsilon 1NH}$ to -$H_{\epsilon 2NH}$, (g) GlnA5-$H_{\epsilon 1NH}$ to -$H_{\epsilon 2NH}$, (h) B3Asn-$H_{\delta 1NH}$ to -$H_{\delta 2NH}$, (i) GlnA15-$H_{\epsilon 1NH}$ to -$H_{\epsilon 2NH}$, (j) impurity, (k) LeuA16-NH to TyrA19-H_ϵ, and (l) TyrB16-H_ϵ to LeuB17-NH. Panel B: (m) PheB25-H_δ to -NH, (n) TyrB26-H_δ to -NH, (o) TyrB16-H_δ to LeuB17-NH, (p) LeuB11-NH to HisB10-NH, (q) SerA9-NH of ThrA8-NH, (r) AsnA21-NH to CysA20-NH, (s) AsnA18-NH to GlnA17-NH, (t) not clear, (u) HisB5-H_δ to -NH, (v) TyrA14-NH to LeuA13-NH, and (w) SerA12-NH to GlnA15-NH.

In such experiments it is important to compare only protons of a given type, e.g., Ala $C_\beta H_3$, Phe H_ϵ, etc. Carr–Purcell–Meiboom–Gill (CPMG) studies of native insulin in 20% deuteroacetic acid demonstrate a large variation in transverse relaxation times (Tables III and IV), which for each type of proton may be classified as follows: (a) *fast*, protons belonging to side chains in the hydrophobic core (such as LeuB15); (b) *intermediate*, protons belong to surface side chains with folded backbone structure (such as HisB10); (c) *slow*, protons belonging to partially disordered regions of the polypeptide chain (such as PheB1). The latter resonances are assigned to the N- and C-termini (A1, A21, B1–B3, B29–B30) and the B-chain β-turn (B20–B23) (Boelens et al., 1990; Hua & Weiss, 1990, 1991). Corresponding CPMG studies of GlyB24-insulin demonstrate that whereas T_2 values of protons in the N-terminal arm (residues B1–B9) are similar to those of native insulin, a systematic trend is observed among residues B22–B30 toward longer relaxation times in the mutant protein (Table III). Longer T_2's are also seen for the methyl resonances of ValB12 and LeuB15 in accord with the relative intensities of their DQF-COSY cross-peaks. In the CPMG series fewer resonances are resolved in the A-chain than in the B-chain (Table IV).

(*ii*) *Pattern of Secondary Shifts.* GlyB24-insulin exhibits significant differences in chemical shifts ($\pm$>0.1 ppm) relative to native insulin (Table II). Such differences may reflect the absence of the PheB24 ring-current field (Kristensen et al., 1991; Weiss et al., 1991) and/or structural perturbations in the mutant protein. Consistent with either mechanism, dispersion of chemical shifts in the spectrum of GlyB24-insulin is less extensive than that of native insulin under the same conditions (Hua & Weiss, 1991). The meta resonances of three tyrosines (A19, B16, and B26), for example, exhibit nearly equivalent chemical shifts in the mutant protein (Table I). Two additional observations are noteworthy. (i) Whereas the chemical shifts of residues B24–B30 in native insulin differ significantly from those of a random-coil peptide corresponding to residues B23–B30 (parts A and B of Table V), the chemical shifts of residues B24–B30 in GlyB24-insulin are similar to those of the corresponding random-coil peptide (part C of Table V; differences in B23 and B24 chemical shifts are presumably due to the inductive effect of the N-terminal TFA group in the peptide). (ii) Whereas in native insulin a unique TyrB26 ortho–meta TOCSY cross-peak is observed, in the spectrum of GlyB24-insulin major (93%) and minor (7%) aromatic cross-peaks are seen (data not shown). A similar

Table I: Chemical Shifts of Assigned ^{1}H-NMR Resonances of GlyB24-Human Insulin in 20% Acetic Acid at 25 °C

		chemical shifts at 25 °C		
residue	NH	$C^\alpha H$	$C^\beta H$	others
A1 Gly		3.97, 3.80		
A2 Ile	8.47	3.86	1.13	$C^\gamma H_2$ 1.13, 0.93
				$C^\gamma H_3$ 0.74, $C^\delta H_3$ 0.63
A3 Val	8.03	3.62	1.92	$C^\gamma H_3$ 0.90, 0.85
A4 Glu	8.08	4.20	2.06, 2.06	$C^\gamma H_2$ 2.48, 2 48
A5 Gln	8.20	4.05	2.06,[b] 2.01[b]	$C^\gamma H_2$ 2.46, 2.38
				$N^\epsilon H_2$ 6.83, 7.50
A6 Cys	8.26	4.88	2.86,[b] 3.31[b]	
A7 Cys	8.27	4.82	3.73,[b] 3.30[b]	
A8 Thr	8.19	4.05	4.39	$C^\gamma H_3$ 1.22
A9 Ser	7.39	4.74	4.01, 3.86	
A10 Ile	7.78	4.37	1.53	$C^\gamma H_2$ 1.09, 0.44
				$C^\gamma H_3$ 0.63, $C^\delta H_3$ 0.51
A11 Cys	9.60	4.88	3.31, 2.86	
A12 Ser	8.71	4.57	3.97,[b] 4.28[b]	
A13 Leu	8.60	3.85	1.34, 1.37	$C^\gamma H$ 1.41, $C^\delta H_3$ 0.78, 0.71
A14 Tyr	7.48	4.14	2.96,[b] 2.88[b]	C2,6H 7.02, C3,5H, 6.79
A15 Gln	7.55	3.95	2.33, 2.00	$C^\gamma H_2$ 2.42, $N^\epsilon H_2$ 6.94, 7.47
A16 Leu	8.06	4.14	1.88, 1.62	$C^\gamma H$ 1.70, $C^\delta H_3$ 0.82, 0.78
A17 Glu	8.06	4.13	2.09, 2.00	$C^\gamma H_2$ 2.56, 2.29
A18 Asn	7.43	4.45	2.57, 2.49	$N^\delta H_2$ 6.50, 7.13
A10 Tyr	7.89	4.48	2.97,[b] 3.29[b]	C2,6H 7.29, C3,5H 6.73
A20 Cys	7.44	4.68	3.25, 2.84	
A21 Asn	8.17	4.74	2.85, 2.77	
B1 Phe		4.27	3.14, 3.14	C2,6H 7.19, C3,5H 7.33
				C4H 7.25
B2 Val	8.13	4.12	1.88	$C^\gamma H_3$ 0.82, 0.82
B3 Asn	8.44	4.69	2.71, 2.71	$N^\delta H_2$ 7.53, 6.91
B4 Gln	8.38	4.46	2.07,[b] 1.88[b]	$C^\gamma H_2$ 2.23, 2.15
				$N^\epsilon H_2$ 7.34, 6.79
B5 His	8.58	4.44	3.23,[b] 3.52[b]	C2H 8.57, C4H 7.40
B6 Leu	8.93	4.48	1.73,[b] 0.93[b]	$C^\gamma H$ 1.56, $C^\delta H_3$ 0.90, 0.74
B 7 Cys	8.29	4.94	3.22, 2.93	
B8 Gly	9.20	3.98, 3.84		
B9 Ser	9.02	4.10	3.87, 3.87	
B10 His	8.00	4.51	3.56,[b] 3.29[b]	C2H 8.69, C4H 7.46
B11 Leu	7.10	4.03	1.86,[b] 1.24[b]	$C^\gamma H$ 1.37, $C^\delta H_3$ 0.83, 0.76
B12 Val	7.21	3.42	2.01	$C^\gamma H_3$ 0.93, 0.85
B13 Glu	7.94	4.07	2.14, 2.05	$C^\gamma H_2$ 2.51
B14 Ala	7.79	4.09	$C^\beta H_3$ 1.48	
B15 Leu	8.13	3.98	1.71, 1.41	$C^\gamma H$ 1.63, C^δH3 0.75, 0.68
B16 Tyr	8.10	4.17	3.10, 3.10	C2,6H 7.05, C3,5H 6.72
B17 Leu	7.88	4.06	1.64,[b] 1.89[b]	$C^\gamma H$ 1.81, $C^\delta H_3$ 0.91, 0.91
B18 Val	8.46	3.87	2.14	$C^\gamma H_3$ 1.03, 0.81
B19 Cys	8.67	4.72	2.85,[b] 3.18[b]	
B20 Gly	7.75	3.88, 3.88		
B21 Glu	7.99	4.28	2.12, 2.01	$C^\gamma H_2$ 2.48, 2.41
B22 Arg	7.97	4.30	1.96, 1.82	$C^\gamma H_2$ 1.66, 1.66
				$C^\delta H_2$ 3.20, 3.20 $N^\epsilon H$ 7.18
B23 Gly	8.11	3.97, 3.92		
B24 Gly	8.03	3.88, 3.88		
B25 Phe	7.91	4.59	2.97, 2.89	C2,6H, 7.07, C3,5H 7.22
				C4H 7.16
B26 Tyr	8.03	4.58	2.89, 2.89	C2,6H 6.99, C3,5H 6.73
B27 Thr	7.83	4.50	4.03	$C^\gamma H_3$ 1.16
B28 Pro		4.36	2.26, 1.90	$C^\gamma H_2$ 1.97, 1.97, $C^\delta H_2$ 3.63
B20 Lys	8.25	4.37	1.83, 1.75	$C^\gamma H_2$ 1.47, $C^\delta H_2$ 1.65
				$C^\epsilon H_2$ 2.96, $N^\epsilon H$ 7.48
B30 Thr	8.04	4.46	4.38	C^γH3 1.15

[a] Chemical shifts are measured relative to the residual CH_3 resonance of acetic acid, presumed to be 2.03 ppm. [b] β resonances for which stereospecific assignment has been obtained.

Table II: Chemical Shift Differences of GlyB24-Insulin and Native Insulin in 20% Acetic Acid at 25 °C (>0.1 ppm)

	chemical shifts at 25 °C			
residue	NH	$C^\alpha H$	$C^\beta H$	others
B11 Leu				$C^\gamma H$ 0.11
B12 Val		0.14		
B14 Ala	0.11			
B15 Leu	0.13	0.16	0.13	$C^\gamma H$ 0.22, $C^\delta H_3$ 0.13, 0.25
B17 Leu	0.10			
B18 Val			0.10	
B21 Glu	–0.37	0.10		
B22 Arg		0.13	–0.10	
B23 Gly	0.47	0.13		
B24 Gly		–0.31		
B25 Phe	–0.29			
B26 Tyr	0.11			
B28 Pro			–0.27	
B30 Thr		0.13		

ratio of major and minor cross-peaks is observed in spectra of the synthetic B23–B30 octapeptides. We ascribe such states to trans and cis isomers of the ThrB27–ProB28 peptide bond. In native insulin the trans configuration is stabilized by packing interactions with the A-chain (Baker et al., 1988; Hua & Weiss, 1991).

Secondary-Structure Analysis. Observation of nested (i,i+3) connectivities and associated strong d_{NN} NOEs demonstrates the existence of three α-helices in the solution structure of GlyB24-insulin: A3–A8, A13–A18, and B9–B19. Similar helix-related NOEs (A2–A8, A12–A18, and B9–B19) are observed in DPI and native insulin (Hua & Weiss, 1990, 1991). The significance of the small difference in A-chain helical end points is unclear. In native insulin residues B20–B23 adopt a (1→4) β-turn, which permits the C-terminal β-strand (B24–B26) to pack against the B-chain α-helix (B9–B19). The presence of the β-turn in native insulin is indicated by local NOEs reflecting the geometry of the β-turn (contacts are observed between ArgB22–H_N and the α protons of GlyB20, and between ArgB22–$H_{\beta 1,2}$ and the α proton of CysB19) and nonlocal NOEs reflecting the B-chain α/β orientation (contacts are observed from PheB24 to ValB12 and TyrB16, and from TyrB26 to LeuB11, ValB12, and LeuB15). None of these NOEs are observed in the spectrum of GlyB24-insulin, suggesting that the β-turn is not stably maintained.

Long-Range NOEs and Tertiary Structure Analysis. The tertiary structure of native insulin consists of an α-helical core and adjoining C-terminal β-strand of the B-chain (residues B24–B28). The folding of these elements in GlyB24-insulin is described in turn.

(*i*) *Tertiary NOEs Define a Native α-Helical Core.* The relative orientations of the three α-helices in GlyB24-insulin are defined by long-range NOEs, which are analogous to those observed in the spectrum of native insulin (Hua & Weiss, 1991). Representative NOEs involving aromatic rings and aliphatic resonances are shown in Figure 9 (the boxed region in panel A is provided in expanded form in the supplementary material). Contacts are observed between IleA2 and TyrA19, between ValA3 and TyrA19, and between IleA10 and HisB5. A2–A19 NOEs demonstrate the proximity of the N- and C-terminal α-helices of the A-chain; A10–B5 NOEs define a local packet between the A-chain and N-terminal (nonhelical) region of the B-chain. Also observed in this region of the NOESY spectrum are (i,i+3) helix-related NOEs between LeuA16 and TyrA19 and (i,i+4) NOEs between ValB12 and TyrB16. Interchain contacts are also observed in each case between the side chains of TyrA19 and LeuB15.

Interchain contacts between AsnA21 and ArgB22 H_β—predicted by crystal structures of native insulin and observed in solution as an AsnA21-N_ϵ/ArgB22 H_β NOE (Hua & Weiss, 1991)—are not observed in the NOESY spectrum of GlyB24-insulin. The absence of this NOE indicates either a stable increase in the A21–B22 distance (i.e., >4.3 Å) or the introduction of subnanosecond fluctuations of the local A21–B22 interproton vectors of sufficient amplitude to quench the NOEs (Wuthrich, 1986).

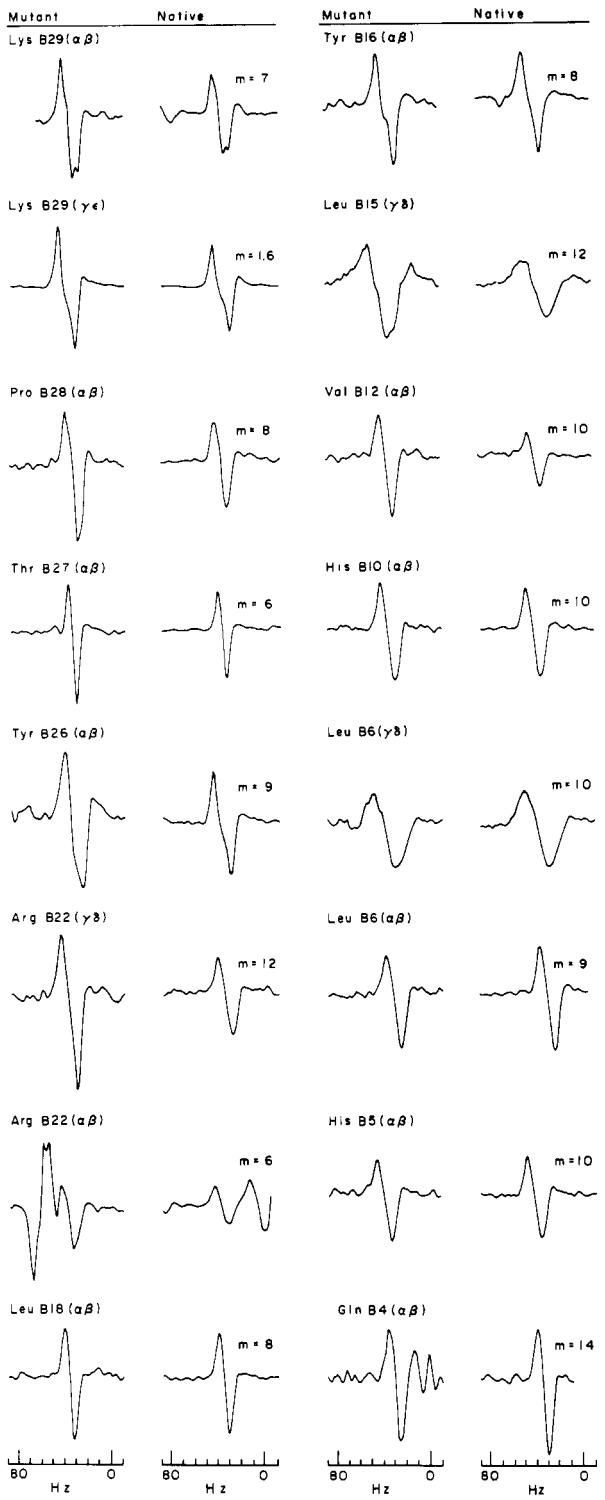

FIGURE 7: Analysis of B-chain DQF-COSY cross-peak intensities. One-dimensional slices are shown through resolved multiplets in the 2D spectra of GlyB24-insulin (left-hand column of each panel) and native human insulin (right-hand column of each panel). Assignments are as indicated. In the mutant protein motional narrowing is evident in the B20–B30 region and those side chains contacted by this region in native insulin (ValB12 and LeuB15; see Figure 9). The two spectra were normalized according to the $\alpha\beta$ cross-peak of TyrA14 (a flexible residue on the surface of the A-chain remote from the site of mutation). For clarity corresponding cross-peaks were scaled by $1/m$ as indicated (i.e., intense signals have low m value, and weak signals have high m value).

(ii) ^{13}C-Isotope-Edited 2D-NMR Studies Demonstrate Disruption of Contacts between the B-chain β-Strand and Hydrophobic Core. In native insulin the aromatic rings of PheB24 and TyrB26 are in van der Waals contact with the side chains of ValB12 and LeuB15. Additional contacts are

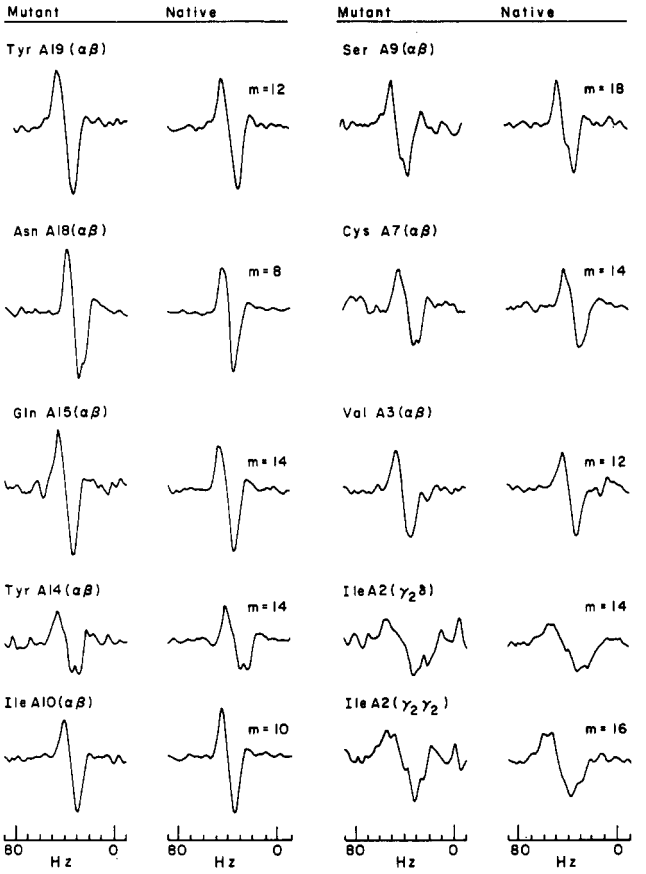

FIGURE 8: Analysis of A-chain DQF-COSY cross-peak intensities. The format is the same as in Figure 7. Some A-chain motional narrowing in GlyB24-insulin is seen, presumably as a transmitted effect of the B-chain perturbation. No narrowing is seen for IleA10 or CysA7, which form an A-chain/B-chain contact remote from the site of mutation.

Table III: Selected Spin–Spin Relaxation Times T_2[a] of B-Chain Resonances

residue	proton	native insulin	mutant insulin
B1	H_ϵ	360	360
B3	H_β	60	70
B5	H_ϵ	390	380
B10	H_δ	440	430
B12	$C_{\gamma 2}H_3$	<120[b]	210
B15	$C_{\delta 2}H_3$	30	120
B18	$C_{\delta 1}H_3$	120	–[c]
B22	H_β	<210	250
B22	H_δ	70	290
B24	H_δ	180	–[c]
B25	H_δ	280	280
B26	H_α	<170[b]	250
B26	H_δ	240	260
B28	H_δ	50	340
B29	H_ϵ	220	410
B30	H_α	–[c]	340
B27/B30[d]	$C^\gamma H_3$	230	320

[a] Values (in ms) obtained by least-squares fit to resolved resonances in 1D CPMG series (Materials and Methods) under conditions in which both the native and mutant proteins are monomeric (37 °C and protein concentration 0.25 mM in 20% acetic acid; Weiss et al., 1989). B22, B27, B29, and B30 side-chain resonances exhibit partial disorder in the native protein (as indicated by relative motional narrowing and absence of significant nonlocal NOEs; Hua & Weiss, 1991) and more complete disorder in the mutant. [b] Composite resonance in 1D spectrum; the most slowly-relaxing component is given as an upper bound. [c] Corresponding resonance cannot be resolved in the 1D NMR spectrum. [d] The $C^\gamma H_3$ resonances of B27 and B30 are degenerate in each spectrum.

Table IV: Selected Spin–Spin Relaxation Times T_2[a] of A-Chain Resonances

residue	proton	native insulin	mutant insulin
A3	H_α	90	–[c]
A5	H_β	80	–[c]
A8	$C_\gamma H_3$	170	300
A10	$C_\delta H_3$	60	50
A12	H_β	70	190
A13	$C_{\delta 1,2} H_3$	–[c]	180
A14	H_ϵ	310	370
A19	H_ϵ	260	440

[a] See footnote to Table III. [b] Composite resonance in 1D spectrum; the most slowly-relaxing component is given as an upper bound. [c] Corresponding resonance cannot be resolved in the 1D NMR spectrum.

Table V: Differences in ^{1}H-NMR Chemical Shifts[a] between Corresponding Protons in Intact Proteins and Synthetic B23–B30 Octapeptides[b]

	H_N	H_α	H_β	other
		(A) Native Insulin (Octapeptide)		
GlyB23[c]		**0.15, 0.15**		
PheB24	**0.25**	**0.40**	**–0.21, –0.22**	$C^\delta H$ **0.19**, $C^\epsilon H$ **0.20**, $C\zeta$ –[d]
PheB25	**–0.14**	–0.05	–0.07, –0.05	$C^\delta H$ 0.00, $C^\epsilon H$ <0.05, $C^\zeta H$ –[d]
TyrB26	**0.07**	–0.04	0.03, 0.03	$C^\delta H$ **0.10**, $C^\epsilon H$ 0.05
TheB27	**0.16**	–0.01	0.00	$C^\gamma H_3$ 0.06
ProB28	–[e]	0.06	**0.12, 0.17**	$C^\gamma H_2$ 0.05, 0.05, $C^\delta H_2$ 0.05
LysB29	**0.09**	**0.04**	0.04, 0.06	$C^\gamma H_2$ 0.08, 0.06, $C^\delta H_2$ 0.06, 0.06 $C^\epsilon H_2$ 0.01, 0.01, $N^\zeta H_2$ 0.05
ThrB30	0.05	**0.10**	0.04	$C^\gamma H_3$ 0.03
		(B) Native Insulin (TFA-Octapeptide)		
GlyB23[f]	**1.71**	**0.12**, 0.06		
PheB24[f]		**0.35**	**–0.24, –0.24**	$C^\delta H$ **0.20**, $C^\epsilon H$ **0.20**, $C^\zeta H$ 0.07
PheB25	**–0.22**	–0.08	**–0.10**, –0.06	$C^\delta H$ –0.03, $C^\epsilon H$ 0.03, $C^\zeta H$ 0.03
TyrB26	0.02	–0.03	0.03, 0.03	$C^\delta H$ **0.10**, $C^\epsilon H$ 0.06
TheB27	**0.12**	–0.01	–0.01	$C^\gamma H_3$ 0.05
ProB28	–[e]	0.07	**0.11, 0.11**	$C^\gamma H_2$ 0.03, 0.03, $C^\delta H_2$ 0.05
LysB29	**1.10**	**0.14**	0.02, 0.04	$C^\gamma H_2$ 0.04, 0.04, $C^\delta H_2$ 0.05, 0.05 $C^\epsilon H_2$ 0.03, 0.03, $N^\zeta H_2$ 0.05
ThrB30	0.09	**0.13**	0.06	$C^\gamma H_3$ –
		(C) Mutant Insulin (TFA-Octapeptide)		
GlyB24[g]	**1.39**	**0.11**		
GlyB24[g]	**0.28**			
PheB25	0.04	–0.04	–0.04, –0.01	C^ζ 0.04
TyrB26			0.04, 0.00	
TheB27				
ProB28				
LysB29	0.03			
ThrB30				

[a] Chemical shift differences greater than or equal to 0.10 ppm are shown in boldface; differences less than 0.2 ppm are omitted. [b] Native B23–B30 octapeptides (GFFYTPKT) were prepared with both free and trifluoroacetylated (TFA) α-amino groups (see Materials and Methods); mutant B23–B30 octapeptide (GGFYTPKT) was prepared as TFA adduct. [c] Chemical shift differences for GlyB23 are likely to reflect the presence of free α-amino group in the octapeptide. [d] Cross-peaks to Phe para resonances are not resolved. [e] Proline does not contain an amide proton. [f] The large perturbations in GlyB23 and PheB24 HN in the TFA adduct are presumably due to the N-terminal TFA protecting group. [g] Comparison of chemical shifts in the native octapeptide ± TFA (parts A and B) indicates that differences in GlyB23 and GlyB24 NH chemical shift are due primarily to the presence of TFA. The observed chemical shifts for B24–B30 in the mutant insulin (Table II) are in accord with random-coil shifts.

made to the A-chain: B26–IleA2, B26–ValA3, and ProB28–ValA3. Because of resonance overlap (Table I), analysis of analogous long-range NOEs in GlyB24-insulin is facilitated by selective ^{13}C labeling of residues B24–B26 ([1,2-$^{13}C_2$]-glycine, [*ring*-$^{13}C_6$]phenylalanine, and [*ring*-$^{13}C_4$]tyrosine). A heteronuclear HMQC spectrum is provided in the supplementary material. In the isotope-edited NOESY spectrum (Figure 10) PheB25 and TyrB26 exhibit only intraresidue NOEs to H_α and H_β resonances. Strikingly, no interresidue NOEs are observed. The two H_α resonances of GlyB24 are

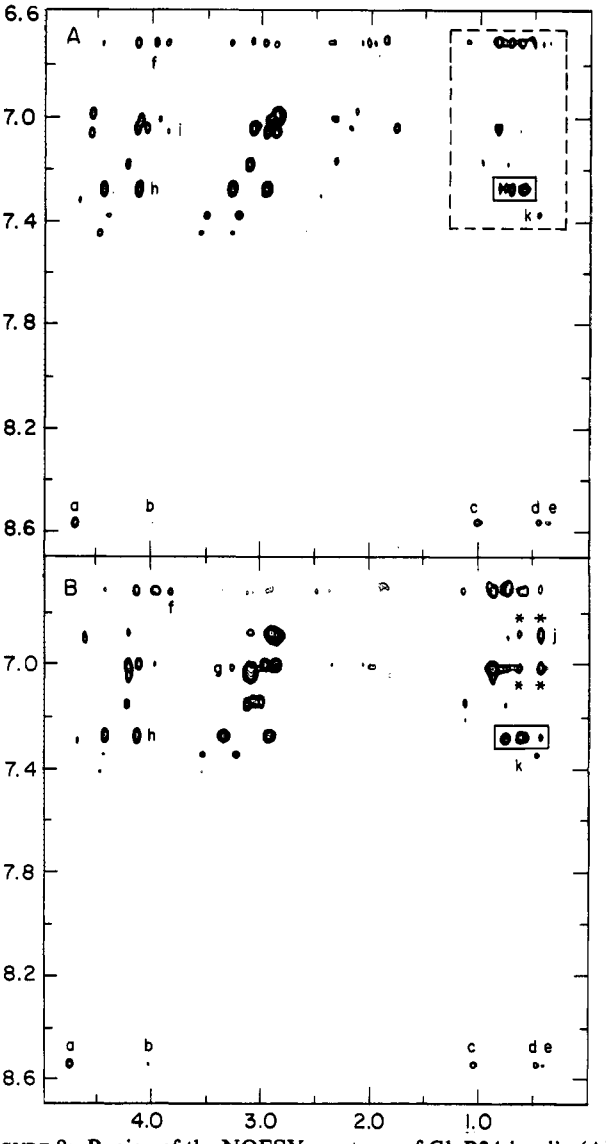

FIGURE 9: Region of the NOESY spectrum of GlyB24-insulin (A) and native human insulin (B) in 20% acetic acid. This region contains cross-peaks between aromatic ring resonances and aliphatic protons and so provides a monitor of the interactions of the C-terminal β-strand of the B-chain (see Figure 12). Important A-chain/B-chain contacts distant to the site of mutation are the same in the two spectra; these are NOEs from HisB5-H_ϵ to SerA9-H_α (cross-peak a in both spectra), to SerA9-$H_{\beta 1}$ (cross-peak b in both spectra), and to IleA10 (cross-peaks c–e in both spectra). The boxed region in panel A is shown in expanded form in the supplemental material, Figure S3. Additional labeled cross-peaks are as follows: (f) TyrA19-meta to LeuB15-H_α; (g, panel B only), PheB24-meta to ValB12-H_α; (h) A19-ortho to LeuA16-H_α; (i, panel A only) PheB25-ortho to GlyB24-H_α; (j, panel B only), PheB24-ortho to LeuB15 methyl; (k) HisB5-H_δ to IleA10-δCH_3. Asterisks in panel B indicate NOEs from the PheB24 ring protons that are absent in the mutant protein.

degenerate (Table I and supplementary material) and also do not exhibit isotope-edited NOEs (data not shown). We note that demonstration of an absent NOE is relative to the obtained signal-to-noise ratio. Any long-range NOEs made by TyrB26 must be reduced by at least 15-fold in intensity relative to those observed from TyrA19. These data do not rule out formation of transient β/α contacts by the mutant protein.

As a control, isotope-edited NOESY studies were also performed under identical conditions with a B26-labeled monomeric insulin analogue with native structure (DKP-insulin; Weiss et al., 1991). As expected, long-range ^{13}C-edited NOEs are observed between the TyrB26 aromatic protons and the α-helical core (ValB12, LeuB15, IleA2, and

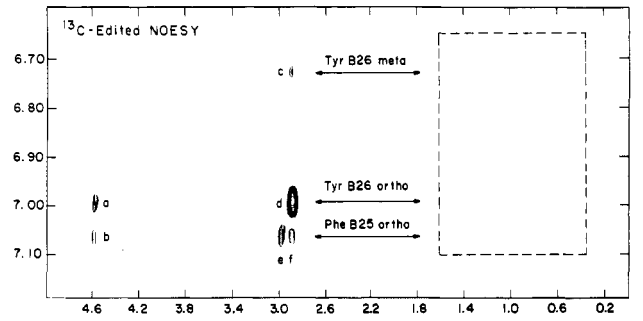

FIGURE 10: ^{13}C-Edited NOESY spectrum of selectively labeled GlyB24-insulin [[$^{13}C_\alpha$]GlyB24, [*ring*-$^{13}C_6$]PheB25, and [*ring*-$^{13}C_4$]-TyrB26) obtained by the method of Bax and Weiss (1987). Boxed region corresponds to that boxed in Figure 9A. Only intraresidue NOEs are observed; nonlocal NOEs to ValB12, LeuB15, IleA2, or ValA3—as predicted by crystal structures and observed in the mutant. Cross-peaks are labeled as follows: (a) TyrB26-ortho to B26-H_α, (b) PheB25-ortho to B25-H_α, (c) TyrB26-meta to B26-H_β, (d) TyrB26-ortho to B26-H_β, (e) PheB25-ortho to B25-$H_{\beta 1}$, and (f) PheB25-ortho to B25-$H_{\beta 2}$.

ValA3). As also expected, an additional weak β-strand/A-chain contact occurs in native insulin between the edge of the ProB28 pyrrolidone ring (H_δ) and a methyl group of ValA3 (Hua & Weiss, 1991); no such NOE is observed in the NOESY spectrum of GlyB24-insulin (data not shown).

(iii) Slowly-Exchanging Amides. Slowly-exchanging H_N resonances are observed over 24 h in D_2O solution (20% deuteroacetic acid), reflecting the presence of stably folded elements of secondary structure. The time course of exchange is presented at 25 °C in Figure 1 (right-hand panel). Slowly-exchanging amide resonances map primarily to the three α-helices. The H_N resonance of GlyB24—unlike that of PheB24 in native insulin (Hua & Weiss, 1991)—is not slowly exchanging. The overall rate of amide proton exchange (among the slowly exchanging subset of protons) is reduced by 67% at 24 h relative to that of DPI (Hua & Weiss, 1990) or intact insulin (Kline & Justice, 1990; Hua & Weiss, 1991).

(III) 2D ^{1}H-NMR Studies in Aqueous Solution

Severe variation in amide linewidths in aqueous–HCl solution leads to multiple ambiguities in the analysis of the "fingerprint" (H_N–H_α) region. Because chemical shifts in aqueous–HCl solution are similar to those in 20% deuteroacetic acid, such ambiguities are readily resolved by analogy to results in 20% deuteroacetic acid.

Analogous Spin-System Identification. In Figure 5 are shown regions of the TOCSY spectra of GlyB24-insulin in 20% deuteroacetic acid (panels A and C) and in aqueous–HCl solution at pH 1.8 (panels B and D). These spectra demonstrate a correspondence of chemical shifts between analogous spin systems. The aromatic spectra are essentially identical (panels C and D).

"Bootstrap" Analysis of Fingerprint Region. The H_N–H_α ("fingerprint") region of the NOESY spectrum of GlyB24-insulin in aqueous–HCl solution is shown in Figure 11; sequential connectivities in the A- and B-chains are delineated in panels A and B, respectively. Chemical shift differences between aqueous–HCl solution and 20% deuteroacetic acid are given in Table VI. Sequential and medium-range contacts are shown in schematic form in the right-hand panels of Figures 3 (A-chain) and 4 (B-chain). Because in each case there are gaps in one or more types of NOE due to amide resonance broadening, it is unlikely that complete assignment could have been obtained in the absence of prior analysis in 20% deuteroacetic acid. Solvent-dependent differences in chemical shift are given in Table VI.

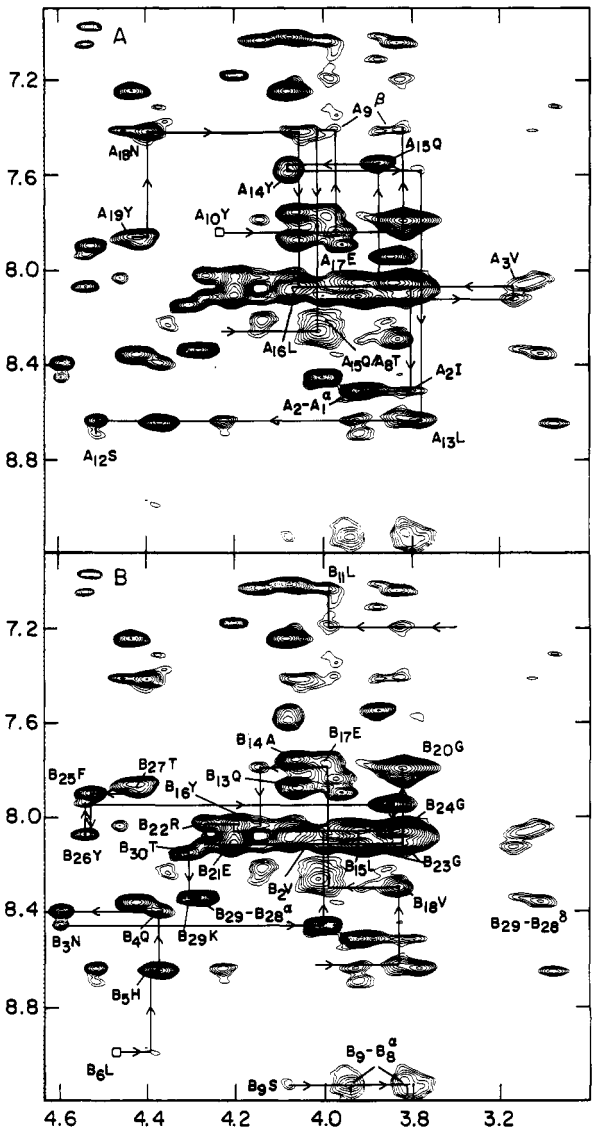

FIGURE 11: Sequential assignment of GlyB24-insulin in aqueous solution (pH 1.8) showing analysis of the "fingerprint" region for the A-chain (panel A) and the B-chain (panel B). These data are summarized in schematic form in Figures 4 and 5, respectively.

Table VI: GlyB24-Insulin Chemical Shift Differences with and without 20% Acetic Acid at 25 °C (>0.1 ppm)

	chemical shifts at 25 °C			
residue	NH	C$^\alpha$H	C$^\beta$H	other
B2 Val		0.12		
B8 Gly	−0.15			
B15 Leu			0.19	
B17 Leu	0.10			
B18 Val	0.16			
B23 Gly		0.10		
B27 Thr		0.10		

Tertiary Structure Is Similar in Aqueous Solution. Since line-broadening in aqueous–HCl solution primarily affects amide resonances (rather than those of carbon-bound protons), NOESY and ^{13}C-edited NOESY spectra are readily obtained in D_2O–DCl (pD 1.9) solution and are essentially identical to those obtained in 20% deuteroacetic acid. In particular, B24–B26–B28 interchain contacts are also absent in aqueous–HCl solution. GlyB24-insulin also exhibits a similar pattern

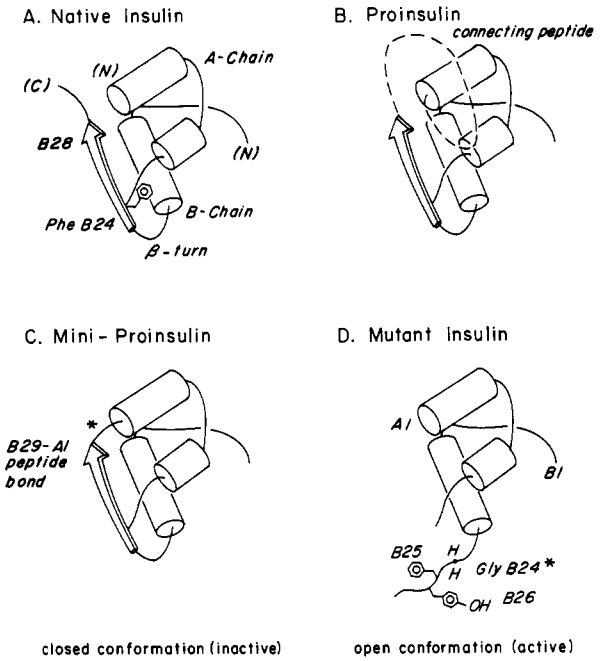

FIGURE 12: (A) Schematic representation of the crystal structure of native insulin (Adams et al., 1969; Peking Insulin Structure Group, 1971). α-Helices are shown as cylinders, and the B-chain C-terminal β-strand is shown as an arrow. The position of PheB24 is indicated. (B) Proinsulin contains an insulin-like moiety and flexible connecting peptide between the N-terminus of the A-chain and C-terminus of the B-chain, as determined by NMR studies (Weiss et al., 1990). A crystal structure of bovine proinsulin has recently been determined; an insulin moiety is observed, but no electron density is observed for most of the connecting peptide (T. L. Blundell, personal communication). (C) Mini-proinsulin is a single-chain insulin analogue containing a peptide bond between B29 and A1 (Markussen, 1986). Its X-ray structure is isomorphic to native insulin in the 4-Zn crystal form (Derewenda et al., 1991). Mini-proinsulin is completely inactive biologically and is proposed to represent the "closed state" of the insulin structure. (D) Proposed model of GlyB24-insulin as an "open state" in which the hydrophobic surface of the N-terminal A-chain α-helix (IleA2–ValA3) is exposed to solvent and presumably also to the insulin receptor.

of slowly exchanging amide resonances in aqueous–DCl solution as in 20% deuteroacetic acid.

DISCUSSION

The mechanism by which insulin binds to its receptor is not understood despite extensive study of insulin's structure in multiple crystal forms (Adams et al., 1969; Peking Insulin Structure Group, 1971; Blundell et al., 1972; Bentley et al., 1978; Smith et al., 1984; Derewenda, et al., 1989; Badger et al., 1991). Structure–function relationships have been probed by comparative studies of species variants (Wood et al., 1975; Emdin et al., 1977; Pullen et al., 1976; Steiner, 1989), diabetes-associated mutant human insulins (Tager et al., 1979; Inouye et al., 1981a,b, 1983; Shoelson et al., 1983a,b, 1984), synthetic or engineered analogues (Inouye et al., 1979, 1982; Assoian et al., 1982; Kobayashi et al., 1982; Fisher et al., 1985; Nakagawa & Tager, 1986, 1987, 1991, 1992; Casaretto et al., 1987; Schwartz et al., 1987; Brange et al., 1988; Schwartz et al., 1989; Mirmira & Tager, 1989, 1991; Mirmira et al., 1991; Wang et al., 1991; Shoelson et al., 1992), and analogues containing chemical cross-links between the A- and B-chains (Brandenburg et al., 1972; Cutfield, et al., 1981, 1986; Nakagawa & Tager, 1989).

Although the major features of insulin crystal structures are retained in solution (Weiss et al., 1989; Kline & Justice, 1990; Boelens et al., 1990; Hua & Weiss, 1990, 1991; Kristensen et al., 1991; Knegtel et al., 1991; Hua et al., 1992), the relevance of these structures (Figure 12A) to the mechanism of receptor binding has recently been challenged. In a pivotal study Derewenda et al. (1991) have determined the crystal structure of a single-chain analogue that contains a main-chain peptide bond between LysB29 and GlyA1 (Markussen, 1985). Because these residues are tethered by a connecting peptide in proinsulin (Figure 12B), the analogue is designated "mini-proinsulin" (Figure 12C). Although mini-proinsulin has no detectable bioactivity, its crystal structure is essentially identical to that of the native insulin. Derewenda et al. (1991) proposed that the structure of mini-proinsulin is "trapped" by the B29–A1 peptide bond in an inactive (closed) state. Presumably, partial separation of the A- and B-chains (the open state) occurs in the hormone–receptor complex.

This proposal predicts the existence of mutant insulins that, as a seeming paradox, retain native potency despite structural perturbations. The B24 position is a possible site of such mutations. In crystal structures the aromatic side chain of the PheB24 makes well-defined tertiary and dimer-related contacts, which would be absent or altered in B24 analogues. Nevertheless, GlyB24-insulin (Mirmira & Tager, 1989) and related B24 analogues containing D-amino acids (Kobayashi et al., 1982; Mirmira & Tager, 1989; Mirmira et al., 1991) exhibit surprisingly high potencies. For this reason we have undertaken 2D-NMR studies of GlyB24-insulin. Unlike native insulin, GlyB24-insulin is monomeric in aqueous–HCl solution. Complete ^{1}H-NMR sequential assignment has been obtained, and tertiary contacts were identified by ^{13}C-edited NOESY experiments. The results demonstrate that the α-helical core is largely retained whereas the C-terminal region of the B-chain (residues B20–B30) undergoes partial unfolding (Figure 12D). Complementary evidence of unfolding is provided by motional narrowing and loss of chemical shift dispersion relative to native insulin.

The near-native bioactivity of GlyB24-insulin suggests that the native B-chain β-turn and β-strand are not required for receptor binding. Nevertheless, our results do not imply that residues B20–B30 are unfolded in the hormone–receptor complex. Indeed, studies of insulin analogues demonstrate that receptor-binding is extremely sensitive to stereochemical features of side chains in this region (Nakagawa & Tager, 1986, 1987; Mirmira & Tager, 1989, 1991; Mirmira et al., 1991). Their importance is also highlighted by the discovery of mutations at positions B24, B25, and A3 in association with diabetes mellitus (Tager et al., 1979; Shoelson et al., 1983a,b; Kobayashi et al., 1984; Haneda et al., 1984, 1985; Nanjo et al., 1987). We imagine that residues B20–B30 adopt a folded but novel configuration in the hormone–receptor complex. In this view the small reduction in the activity of GlyB24-insulin would be largely due to the entropic cost of stabilizing a disordered region on receptor binding. Loss of function in diabetes-associated mutant insulins PheB24→Ser and PheB25→Leu may reflect either an impaired ability to adopt the bound-state structure or a perturbed receptor contact in the bound state.

Changes in B-chain structure can propagate to the A-chain. In crystal and solution structures of native insulin, for example, the B-chain β-strand limits the accessibility of A-chain residues IleA2 and ValA3. By contrast, in GlyB24-insulin and in crystal structures of des-pentapeptide(B26–B30)-insulin (DPI; Bi et al., 1984; Dai et al., 1987) these hydrophobic side chains are exposed and thus accessible for direct interaction with the receptor. This possibility is in accord with functional studies of insulin analogues: residues A2 and A3 are critical (Okada

et al., 1981; Kitagawa et al., 1984; Inouye et al., 1985; Nanjo et al., 1986; Kobayashi et al., 1986; Nakagawa & Tager, 1992) whereas residues B26–B30 are not (Fisher et al., 1985; Nakagawa & Tager, 1986). If the IleA2 and ValA3 side chains function as "knobs in holes", then the defect in diabetes-associated mutant insulin ValA3→Leu (Nanjo et al., 1986) would be in a receptor contact rather than be mediated by nonlocal perturbations in insulin's structure.

How far from the A-chain is the B-chain C-terminus in the hormone–receptor complex? The question has been indirectly probed by chemical cross-linking of the ϵ-NH_2 group of LysB29 to the α-NH_2 group of GlyA1 with reagents of different lengths (Cutfield et al., 1981; Nakagawa & Tager, 1989). Although a general trend is observed wherein longer tethers are associated with high bioactivity, one tightly constrained analogue (containing the two-carbon oxaloyl cross-link) exhibits anomalously high bioactivity relative to a less constrained analogue (containing the four-carbon succinoyl cross-link; Nakagawa & Tager, 1989). The oxaloyl derivative also exhibits an altered near-UV CD spectrum (Brandenburg et al., 1972), and so its increased relative potency may reflect a distorted conformation that mimics aspects of insulin's receptor-bound conformation (Brems et al., 1991). The crystal or solution structures of the oxaloyl and succinoyl derivatives have not been determined.

In summary, we have described isotope-aided 2D-NMR studies of an anomalous mutant insulin (GlyB24-insulin), which exhibits partial unfolding of B-chain residues B20–B30. The results support the intriguing possibility that these residues adopt a novel configuration in the hormone–receptor complex (Derewenda et al., 1991; Hua et al., 1991). Limitations of the present study define key issues for future investigation. First, the present data provide only a qualitative view of protein dynamics. Heteronuclear NMR relaxation studies of ^{15}N- or $^{13}C_\alpha$-labeled insulin analogues in conjunction with molecular dynamics simulations may in the future permit quantitative analysis of subnanosecond main-chain fluctuations (Chandrasekhar et al., 1992). Second, the present results do not define the extent of conformational space that is sampled by residues B20–B30. A "random" sampling of possible configurations, as would be given for example by distance–geometry algorithms in the absence of input restraints (Hua et al., 1991), is unlikely to have a physical meaning. Third, the structure of insulin at the receptor surface remains an outstanding unsolved problem. Insight toward defining a pharmacophore of the receptor-bound state may emerge from studies of high-potency analogues (Kobayashi et al., 1982; Mirmira & Tager, 1989; Mirmira et al., 1991) that—unlike GlyB24-insulin—adopt a stable but nonnative structure.

ACKNOWLEDGMENT

We thank R. E. Chance (Eli Lilly & Co.) for des-octapeptide-insulin and advice; J. Lee, M. Kochoyan (Harvard Medical School), P. E. Wright (Research Institute of the Scripps Clinic), A. Bax (NIH), W. M. Westler (University of Wisconsin, Madison), and a reviewer for helpful discussion concerning NMR techniques; C. S. Lynch and M. Chaudhuri for peptide synthesis and semisynthesis; Wenhua Jia for NMR processing and plotting; G. G. Dodson and T. L. Blundell for communicating results prior to publication; J. Avruch, T. L. Blundell, M. Dunn, G. G. Dodson, C. R. Kahn, and G. Wagner for helpful discussion; and L. J. Neuringer (MIT) for support in the early stages of the work. We thank Prof. Christopher T. Walsh, Elkan Blout, Eugene Braunwald, and John T. Potts, Jr., for their encouragement.

SUPPLEMENTARY MATERIAL AVAILABLE

Aromatic regions of DQF-COSY spectra of native and GlyB24-insulins (Figure S1); ^1H–^{13}C HMQC spectrum of selectively labeled GlyB24-insulin (Figure S2); and expanded section of NOESY spectrum of GlyB24-insulin showing long-range NOEs (Figure S3) (4 pages). Ordering information is given on any current masthead page.

REFERENCES

Adams, M. J., Blundell, T. L., Dodson, E. J., Dodson, G. G., Vijayan, M., Baker, E. N., Hardine, M. M., Hodgkin, D. C., Rimer, B., & Sheet, S. (1969) *Nature (London) 224*, 491–495.

Assoian, R. K., Thomas, N. E., Kaiser, E. T., & Tager, H. S. (1982) *Proc. Natl. Acad. Sci. U.S.A. 79*, 5147–5151.

Badger, J., Harris, M. R., Reynolds, C. D., Evans, A. C., Dodson, E. J., Dodson, G. G., & North, A. C. T. (1991) *Acta Crystallogr. B46*, 127–136.

Baker, E. N., Blundell, T. E., Cutfield, G. S., Cutfield, S. M., Dodson, E. J., Dodson, G. G., Hodgkin, D. M. C., Hubbard, R. E., Iassac, M. W., Reynolds, D. C., Sakabe, K. S., Sakabe, N., & Vjayan, N. M. (1988) *Philos. Trans. R. Soc. London, B 319*, 389–456.

Bax, A., & Weiss, M. A. (1987) *J. Magn. Reson. 71*, 571–575.

Bentley, G., Dodson, G., & Lewitova, A. (1978) *J. Mol. Biol. 126*, 871–875.

Bi, R. C., Dauter, Z., Dodson, E., Dodson, G., Giordano, F., & Reynolds, C. (1984) *Biopolymers 23*, 391–395.

Blundell, T. L., & Humbel, R. E. (1980) *Nature (London) 287*, 781–787.

Blundell, T. L., Dondson, G. G., Hodgkin, D. C., & Mercola, D. A. (1972) *Adv. Protein Chem. 26*, 279–402.

Boelens, R., Ganadu, M. L., Verheyden, P., & Kaptein, R. (1990) *Eur. J. Biochem. 191*, 147–153.

Brandenburg, D., Busse, W.-D., Gattner, H.-G., Zahn, H., Wollmer, A., Gliemann, J., & Puls, W. (1972) in *Proceedings of the 12th European Peptide Symposium* (Hanson, H., & Jakubke, H.-D., Eds.) pp 270–283, North Holland, Amsterdam.

Brange, J., Ribel, U., Hansen, J. F., Dodson, G., Hansen, M. T., Havelund, S., Melberg, S. G., Norris, F., Norris, K., Snel, L., Sorensen, A. R., & Voigt, H. O. (1988) *Nature 333*, 679–682.

Brems, D. N., Brown, P. L., Nakagawa, S. H., & Tager, H. S. (1991) *J. Biol. Chem. 266*, 1611–1615.

Casaretto, M., Spoden, M., Diaconescu, C., Gattner, H.-G., Zahn, H., Brandenburg, D., & Wollmer A. (1987) *Biol. Chem. Hoppe-Seyler 368*, 709–716.

Chandrasekhar, I., Clore, G. M., Szabo, A., Gronenborn, A. M., & Brooks, B. R. (1992) *J. Mol. Biol. 226*, 239–250.

Cheshnovsky, D., Neuringer, L. J., & Williamson, K. L. (1983) *J. Protein Chem. 2*, 335–339.

Chothia, C., Lesk, A. M., Dodson, G. G., & Hodgkin, D. C. (1983) *Nature 302*, 500–505.

Cutfield, J., Cutfield, S., Dodson, E., Dodson, G., Hodgkin, D., & Reynolds, C. (1981) *Hoppe-Seyler's Z. Physiol. Chem. 262*, 755–761.

Cutfield, S. M., Dodson, G. G., Ronco, N., & Cutfield, J. F. (1986) *Int. J. Peptide Protein Res. 27*, 335–343.

Dai, J.-B., Lou, M.-Z., You, J.-M., & Liang, D.-C. (1987) *Sci. Sin. 30* (1), 55–65.

Derewenda, U., Derewenda, Z., Dodson, E. J., Dodson, G. G., Reynolds, C. D., Smith, G. D., Sparks, C., & Swenson, D. (1989) *Nature 338*, 594–596.

Derewenda, U., Derewenda, Z., Dodson, E. J., Dodson, G. G., Bing, X., & Markussen, J. (1991) *J. Mol. Biol. 256*, 1406–1412.

Dodson, E. J., Dodson, G. G., & Hodgkin, D. C. (1979) *Can. J. Biochem. 57*, 469–479.

Emdin, S. O., Gammeltoft, S., & Gliemann, J. (1977) *J. Biol. Chem. 252*, 602–608.

Fischer, W. H., Saunders, D., Brandenburg, D., Wollmer, A., & Zahn, H. (1985) *Hoppe-Seyler's Z. Biol. Chem. 366*, 521–525.

Fischer, W. H., Saunders, D., Diaconescu, C., Brandenburg, D., Wollmer, A., Dodson, G., De Meyts, P., & Zahn, H. (1986) *Hoppe-Seyler's Z. Biol. Chem. 367*, 999–1006.

Goldman, J., & Carpenter, F. H. (1974) *Biochemistry 13*, 4566–4574.

Haneda, M., Polonsky, K. S., Bergenstal, R. M., Jaspan, J. B., Shoelson, S. E., Blix, P. M., Chan, S. J., Kwok, S. C. M., Wishner, W. B., Zeidler, A., Olefsky, J., M., Freidenberg, G., Tager, H. S., Steiner, D. F., & Rubenstein, A. H. (1984) *N. Engl. J. Med. 310*, 1288–1294.

Haneda, M., Kobayashi, M., Maegawa, H., Watanabe, N., Takata, Y., Ishibashi, O., Shigeta, Y., & Inouye, K. (1985) *Diabetes 34*, 568–573.

Hua, Q. X., & Weiss, M. A. (1990) *Biochemistry 29*, 10545–10555.

Hua, Q. X., & Weiss, M. A. (1991) *Biochemistry 30*, 5505–5515.

Hua, Q. X., Shoelson, S. E., Kochoyan, M., & Weiss, M. A. (1991) *Nature 354*, 238–241.

Hua, Q. X., Kochoyan, M., & Weiss, M. A. (1992) *Proc. Natl. Acad. Sci. U.S.A. 89*, 2379–2383.

Inouye, K., Watanabe, K., Morihara, K., Tochino, Y., Kanaya, T., Emura, J., & Sakakibara, S. (1978) *J. Am. Chem. Soc. 101*, 751–752.

Inouye, K., Watanabe, K., Tochino, Y., Kobayashi, M., & Shigeta, Y. (1981a) *Biopolymers 20*, 1845–1858.

Inouye, K., Watanabe, K., Tochino, Y., Kanaya, T., Kobayashi, M., & Shigeta, Y. (1981b) *Experientia 37*, 811–813.

Inouye, K., Watanabe, K., Tochino, Y., Kobayashi, M., & Shigeta, Y. (1983) in *Peptide Chemistry 1982* (Sakakibara, S., Ed.) pp 277–282, Protein Research Foundation, Osaka, Japan.

Kline, A. D., & Justice, R. M., Jr. (1990) *Biochemistry 29*, 2906–2913.

Kitagawa, K., Ogawa, H., Burke, G. T., Chanley, J. D., & Katsoyannis, P. G. (1984) *Biochemistry 23*, 1405–1413.

Kobayashi, M., Ohgaku, S., Iwasaki, M., Maegawa, H., Shigeta, Y., & Inouye, K., (1982) *Biochem. Biophys. Res. Commun. 107*, 329–336.

Kobayashi, M., Ohgaku, S., Iwasaki, M., Maegawa, H., Shigeta, Y., & Inouye, K. (1984) *Biochem. Biophys. Res. Commun. 119*, 49–57.

Kobayashi, M., Takata, Y., Ishibashi, O., Sasaoka, T., Iwasaki, M., Shigeta, Y., & Inouye, K. (1986) *Biochem. Biophys. Res. Commun. 137*, 250–257.

Kristensen, S. M., Jorgensen, A. M., Led, J. J., Balschmidt, P., & Hansen, F. B. (1991) *J. Mol. Biol. 218*, 221–231.

Markussen, J. (1985) *Int. J. Peptide Protein Res. 26*, 70–77.

Markussen, J., Diers, I., Hougaard, P., Langkjaer, L., Norris, K., Snel, L., Melberg, S. G., & Johnson, W. C. (1990) *Proteins 8*, 280–286.

Melberg, S. G., & Johnson, W. C., Jr. (1990) *Proteins: Struct., Funct., Genet. 8*, 280.

Mirmira, R., & Tager, H. S. (1989) *J. Biol. Chem. 264*, 6349–6354.

Mirmira, R., & Tager, H. S. (1991) *Biochemistry 30*, 8222–8229.

Mirmira, R., Nakagawa, S. H., & Tager, H. S. (1989) *J. Biol. Chem. 266*, 1428–1436.

Nakagawa, S. H., & Tager, H. S. (1986) *J. Biol. Chem. 261*, 7332–7341.

Nakagawa, S. H., & Tager, H. S. (1987) *J. Biol. Chem. 262*, 12045–12058.

Nakagawa, S. H., & Tager, H. S. (1989) *J. Biol. Chem. 264*, 272–279.

Nakagawa, S. H., & Tager, H. S. (1992) *Biochemistry 31*, 3204–3214.

Nanjo, K., Snake, T., Miyano, M., Okai, K., Sowa, R., Kondo, M., Nishimura, S., Iua, K., Miyurama, I. C., Given, B. D., Chan, S. J., Tager, H., Steiner, D., & Rubinstein, A. (1986) *J. Clin. Invest. 77*, 514–519.

Okada, Y., Chanley, J. D., Burke, G. T., & Katsoyannis, P. G. (1981) *Hoppe-Seyler's Z. Physiol. Chem. 362*, 629–638.

Peking Insulin Structure Group (1971) *Peking Rev. 40*, 11–16.

Pullen, R. A., Lindsay, D. G., Wood, S. P., Tickle, I. J., Blundell, T. L., Wollmer, A., Krail, A., Brandenburg, D., Zahn, H., Gliemann, J., & Gammeltoft, S. (1976) *Nature (London) 259*, 369–373.

Roy, M., Lee, R. W.-K., Brange, J., & Dunn, M. F. (1990) *J. Biol. Chem. 265*, 5448–5453.

Schwartz, G. P., Burke, G. T., & Katsoyannis, P. G. (1989) *Proc. Natl. Acad. Sci. U.S.A. 86*, 458–461.

Shoelson, S. E., Haneda, M., Blix, P., Nanjo, K., Sanke, T., Inouye, K., Steiner, D., Rubenstein, A., & Tager, H. (1983a) *Nature (London) 302*, 540–542.

Shoelson, S. E., Fickova, M., Haneda, M., Nahum, A., Musso, G., Kaiser, E. T., Rubenstein, A. H., & Tager, H. (1983b) *Proc. Natl. Acad. Sci. U.S.A. 80*, 7390–7394.

Shoelson, S. E., Lu, Z.-X., Parlavtan, L., Lynch, C. S., & Weiss, M. A. (1992) *Biochemistry 31*, 1757–1767.

Smith, G. D., Swenson, D. C., Dodson, G. G., & Reynolds, C. D. (1984) *Proc. Natl. Acad. Sci. U.S.A. 81*, 7093–7097.

Steiner, D. F., Chan, S. J., Welsh, J. M., & Kwok, S. C. M. (1985) *Annu. Rev. Genet. 19*, 463–484.

Steiner, D. F., Bell, G. I., & Tager, H. S. (1990) in *Endocrinology* (DeGroot, L. J., Ed.) pp 1263–1289, W. S. Saunders Co., Philadelphia, PA.

Tager, H., Given, B., Baldwin, D., Mako, M., Markese, J., Rubenstein, A., Olefsky, J., Kobayashi, M., Kolterman, O., & Poucher, R. (1979) *Nature (London) 281*, 122–125.

Wang, S.-h., Hu, S.-q., Burke, G. T., & Katsoyannis, P. G. (1991) *J. Protein Chem. 10*, 313–324.

Weiss, M. A., Eliason, J., & States, D. J. (1984) *Proc. Natl. Acad. Sci. U.S.A. 81*, 6019–6023.

Weiss, M. A., Nguyen, D. T., Khait, I., Inouye, K., Frank, B. H., Beckage, M., O'Shea, E. K., Shoelson, S. E., Karplus, M., & Neuringer, L. J. (1989) *Biochemistry 29*, 9855–9873.

Weiss, M. A., Hua, Q. X., Frank, B. H., Lynch, C. S., & Shoelson, S. E. (1991) *Biochemistry 30*, 7373–7389.

Wood, S. P., Blundell, T. L., Wollmer, A., Lazarus, N. R., & Neville, R. W. J. (1975) *Eur. J. Biochem. 55*, 531–542.

Wuthrich, K. (1986) *NMR of Proteins and Nucleic Acids*, Wiley & Sons, New York, NY.